Journal of Imaging Science and Technology® 50(6): 572–582, 2006.

Image Format for Spectral Image Browsing

Markku Hauta-Kasari▲, Juha Lehtonen and Jussi Parkkinen▲
Department of Computer Science and Statistics, University of Joensuu, P.O. Box 111, FIN-80101 Joensuu, Finland
E-mail: juha.lehtonen@cs.joensuu.fi

Timo Jaaskelainen▲
Department of Physics and Mathematics, University of Joensuu, P.O. Box 111, FIN-80101 Joensuu, Finland

Abstract. *The technology for spectral imaging has developed rapidly during the past few years. The spectral cameras are usable in a variety of applications. These applications include archiving of artistic and museum objects, telemedicine, and e-commerce. In all of these applications, a large number of images will be stored in the archives with a high spatial and spectral (color) resolution. A possibility for fast browsing of these archives is needed. For browsing, the speed is more important than the high resolution of the images. The original, high resolution spectral images should be kept in the archive. In this paper, the authors present a new spectral image browsing architecture. This architecture contains a new data structure for spectral images. The data structure is based on a low-dimensional representation of original spectral images including a spatial subsampling of eigenimages. The authors show that this format enables fast network transfer of spectral images with a small loss of spatial and spectral information. Also, measures of visual quality are given. © 2006 Society for Imaging Science and Technology.* [DOI: 10.2352/J.ImagingSci.Technol.(2006)50:6(572)]

INTRODUCTION

Spectral imaging technology and its applications are under rapid development. Present imaging representation and display techniques for color images are mainly based on three-dimensional color coordinate systems. In computer applications, a RGB-system is mostly used. However, new application areas like telemedicine, e-commerce, and archiving of images of cultural heritage objects are evolving.[1] Some problems with RGB-images in these applications are that one cannot, e.g., manage the change of an object's color under different illuminations or the accurate color of an object cannot be determined. Display technology also causes a problem: all the desired colors cannot be displayed due to the limitation of the device depended color gamut.[2] Metamerism is a phenomenon where two objects look the same under one illumination but different under another one. This is due to the limited ability of the three-dimensional color coordinate system to express colors, but can be overcome by using spectra for object color representation.[3,4] In some applications, especially in telemedicine and e-commerce, the managing of changes in illumination is important. This is a relevant problem since an image is taken under one illumination and viewed after transfer under another illumination. If RGB-colors are used, it is impossible to accurately estimate the color under a different illumination. Hence, the full spectral information of color is needed.

To overcome the above mentioned problems, various spectral image processing and display systems have been developed. In these systems, the color image is represented by n component images, where n can value up to a few hundred. The RGB-image can be seen as a special case where n equals 3.

In spectral image acquisition, six basic methodologies are used. In interference filter based systems the component images are acquired one by one as regular gray-level images through narrow band interference filters.[5,6] In this system, a component image is taken as one shot and the system scans during image acquisition over the spectral region. The object should stay stable during the scanning. Liquid crystal tunable filter[6,7] (LCTF) electronically scans the spectral region and is faster than the mechanically scanned interference filter wheel. The grating based imagers are line scanners, where for one line in the object the whole spectrum of each pixel is captured. The final spectral image is acquired by spatial scanning over the whole object.[8] Also, this is a narrowband type imaging system. The fourth system construction also uses gratings for spectral dispersion, but either optical or temporal integration is used for producing an arbitrary broadband filter for component image acquisition. In this system, the component images are spatially accurate and the spectrum is scanned corresponding to the number of filters.[9,10] Acousto-optic tunable filters can also be used to scan the spectral region.[11] Interferometry based devices are also developed, e.g., SpectraCube.[12] The basic characteristics of the spectral imaging systems are summarized in Table I.

Unlike spectral imaging systems, there are no spectral display systems commercially available at the moment. However, there is ongoing research in projective multiprimary systems,[1,13] e.g., in the Tokyo Institute of Technology. Also in printing technology, methods using more than four primary colors are under intensive research.[14] Presently, published multiprimary display systems use six relatively narrow band filters in front of white light to produce six primary colors. The system enables the display of the spectral colors more

▲IS&T Member

Received Dec. 12, 2005; accepted for publication Mar. 9, 2006.
1062-3701/2006/50(6)/572/11/$20.00.

Table I. Characteristics of spectral imaging systems.

	Interference filters	LCTF[a]	PGP[b]	LVF/LCSLM[c] system	AOTF[d]	Interferometric[e]
Filter type	Narrow band	Narrow/ broadband[f]	Narrow band	Narrow/ broadband[f]	Narrow band	Narrow band
Number of filters	16–40	6–61	60–420	4–8	20–40	80
Scanning direction	Spectral	Spectral	Spatial	Spectral	Spectral	Spectral
Acquisition time	Slow	Fast	Medium	Slow/fast	Fast	Fast
Scanning type	Mechanical	Electrical	Mechanical	Electrical/ mechanical	Electrical	Electrical
Sensor	CCD[g]	CCD	CCD	CCD	CCD	CCD
Spatial resolution	Fixed, CCD-dep.	Fixed, CCD-dep.	Scanning dependent	Fixed, CCD-dep.	AOTF, CCD-dep.	Fixed, CCD-dep.
Spectral resolution	Fixed, filter-dep.	Fixed, filter-dep.	Fixed CCD-dep.	Computational	AOTF-dep.	Optics-dep.

[a]Liquid crystal tunable filter.
[b]Prism-grating-prism (ImSpector).
[c]Linear variable filter/liquid crystal spatial light modulator (See Refs. 9 and 10).
[d]Acousto-optical tunable filter.
[e]SpectraCube.
[f]Adjustable.
[g]Charge coupled device.

accurately than RGB and offers better coverage over the color space, i.e., the display gamut is wider than in RGB-displays.[1] First attempts toward moving spectral images have been taken in Ref. 15, and also a six-primary channel video camera is developed.[16] In addition, there has been a lot of improvement in sensor technology that will provide control over the illuminant variety and retune the display automatically.[17]

Hardware development means that there is a need for spectral image processing and analyzing methods. The spectral images have large memory requirements, which set the needs for image compression and data reduction. This is an especially considerable issue in the browsing of large databases. Examples of the memory requirements are shown in Table II.

Table II. Memory requirements for different image formats.

Image type (8 bits/pixel)	256×256 pixels	512×512 pixels
Gray level image	64 kB	256 kB
RGB image	192 kB	768 kB
Spectral image (20 nm resol.)[a]	1 MB	4 MB
Spectral image (5 nm resol.)[a]	4 MB	16 MB
Moving spectral image (10 s, 20 nm resol.)[a,b]	246 MB	983 MB

[a]400–700 nm.
[b]24 frames/s.

There are some projects in art museums to store spectral images of paintings into the database.[18] For example, in the National Gallery (UK) spectral information about color changes in paintings has been collected since late 1980s, as well as an archive of spectral images of paintings. In general, art museums around the world are going to use digital technology for archiving and conservation purposes. This development also sets the needs for new methods of spectral image processing. We belive that there will be spectral image archives also in other fields, like the cosmetics industry and telemedicine.[19] However, many techniques in color image transmission are bound to the traditional RGB representation. The need for spectral image compression is becoming more and more important to avoid inefficient data communications.[20–23]

In this paper, we consider the situation of several spectral image archives in a network. One needs to browse the images to find a desirable one. This preliminary browsing does not require the full resolution image representation. We describe a novel browsing architecture including an image compression format for the fast browsing of spectral images with good visual quality.

The paper is organized as follows: In the section Spectral Image Browsing Architecture, an architecture for constructing a system for spectral image browsing is described. The section Image Formats overviews the methods for in-

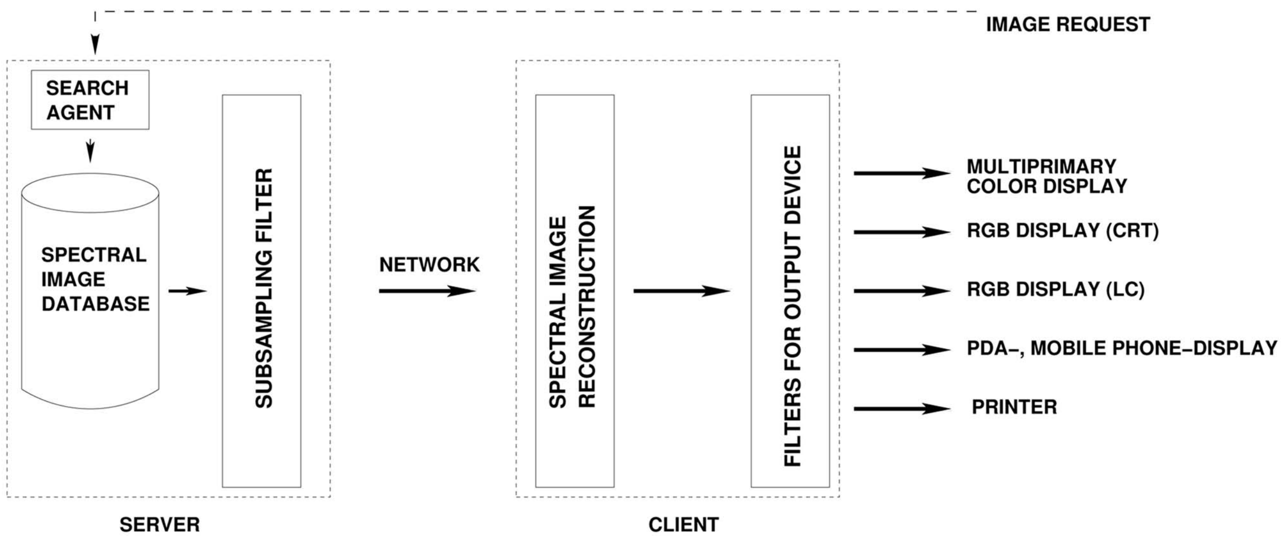

Figure 1. Spectral image browsing architecture.

formation compression in spectral domain and gives a new compression format for spectral images. The section Experimental Results contains experimental results of the usefulness and accuracy of the proposed format. The section Discussion concludes the results and includes a discussion about the future developments and special constraints for the proposed technology.

SPECTRAL IMAGE BROWSING ARCHITECTURE

In this study, we consider the following situation. There are spectral images stored in the spectral image archive. The images may be saved either in raw spectral image format or in principal component analysis (PCA) component image format. Image formats are explained in detail in the Image Formats section. The systems utilize a client-server model for browsing. The client sends a request to the image archive, which is located in a spectral image server. The actual database search is realized by an intelligent agent which also recognizes the image format. When the agent returns the image, it is sent to the client.

In browsing, the image should not be presented in the highest resolution. The most important feature is the communication speed. Therefore, the images have been archived also to the lower spectral resolution browsing format which is still visually acceptable. This transformed image is sent to the client. At the client, there may be many different types of displays from high quality multiprimary color displays to low-resolution PDA's. Before the display, the spectral image is reconstructed and this image is driven through a display filter to match the display characteristics. The architecture is shown in Fig. 1. A subsampling filter and spectral reconstruction are explained in detail below.

IMAGE FORMATS

As described above, spectral representation of color images has many advantages over the RGB presentation. It is also clear that preserving the full spectral information is memory consuming. There are some techniques in the literature to compress the color spectra while preserving information about the raw spectrum sufficiently. These methods include PCA (Refs. 24–26) and independent component analysis[27,28] (ICA). Also a similar encoding format conventionally compatible for today's monitors and printers has been established, where the first three values define the tristimulus model and additional channels are added for defining the spectrum more accurately.[29] From these studies, one may conclude that the color spectra can be reconstructed in relatively high accuracy by using 5–10 basis vectors. The image can also be stored in the PCA or ICA transformed format. PCA eigenimages can be compressed, e.g., with JPEG compression.[26]

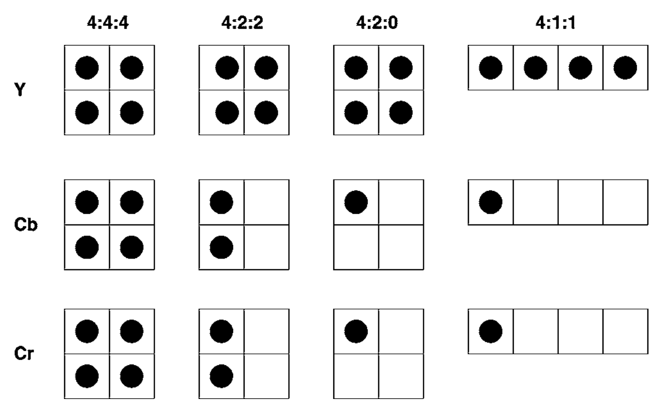

Figure 2. Subsampling schemes in which the selected pixels are shown as black circles inside 2×2 pixels blocks (methods 4:2:2 and 4:2:0) and inside 1×4 pixels block (method 4:1:1). Method 4:4:4 means that there is no spatial compression done.

It is known that the human visual system is more sensitive to spatial resolution in an achromatic channel than in chromatic channels.[30] This fact has been utilized in color image transform and compression methods. For example, in the PAL TV-system and in the JPEG compression method, the colors are represented by YCbCr coordinates, where Y is

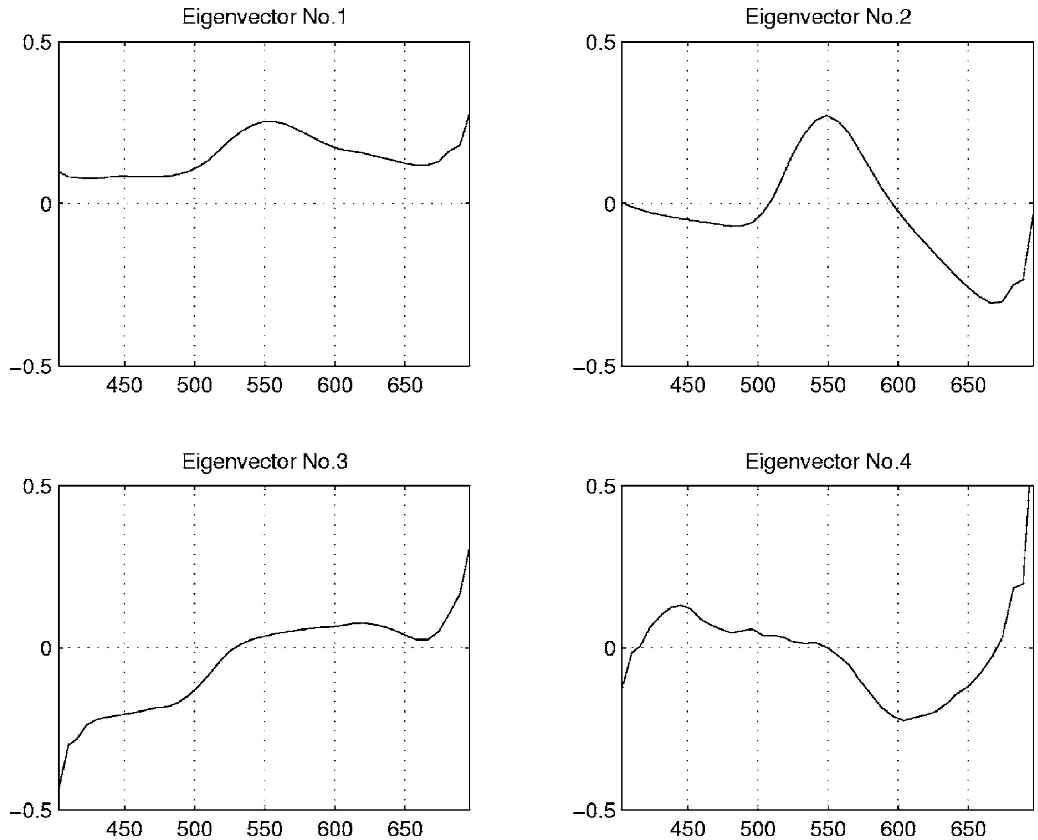

Figure 3. The eigenvectors of PCA for Park2-spectral image in the FOREST database.

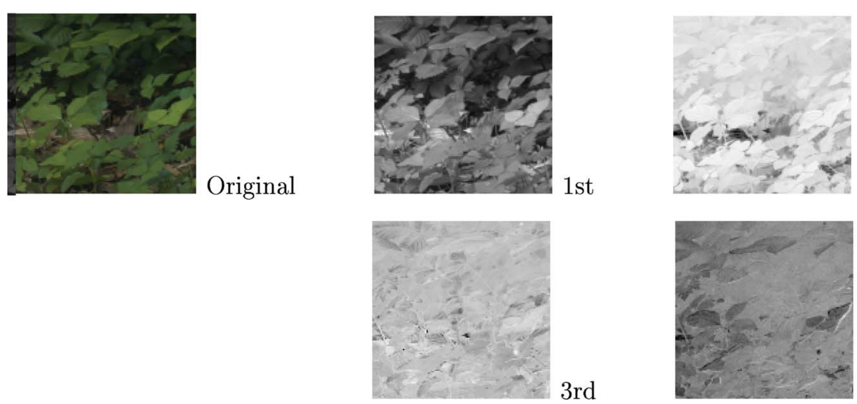

Figure 4. The spectral image (Park2) and the eigenimages. Original image is shown in color in Fig. 6.

the achromatic information, while Cb and Cr carry the chromatic information of the color. In these methodologies, spatial compression of chromatic channels has been utilized by subsampling the Cb and Cr channels.[31]

Subsampling is realized using the standard 4:2:2, 4:2:0, and 4:1:1 subsampling schemes for sampling every second or every fourth pixel from the Cb and Cr component images.[31] The idea of these subsampling methods is shown in Fig. 2, in which the selected pixels are shown as black circles inside 2×2 pixel blocks (methods 4:2:2 and 4:2:0) and inside 1×4 pixel blocks (method 4:1:1). Method 4:4:4 means that spatial compression is not done. Here $A:B:C$ describes a block of $1\times A$ pixels, where B pixels are selected from every block in odd rows and C pixels are selected from every block in even rows.

In this study, we apply the subsampling idea into an expanded eigenimage representation. After computing PCA eigenvectors from a spectral image, one can represent the spectral image by a set of eigenimages, which are formed by computing the inner product between the pixel spectrum and each eigenvector. The first of these eigenimages contains average scalar information of the spectra.

Figure 3 shows the first four eigenvectors of the PCA for one spectral image (Park2) in the FOREST database.[32] In

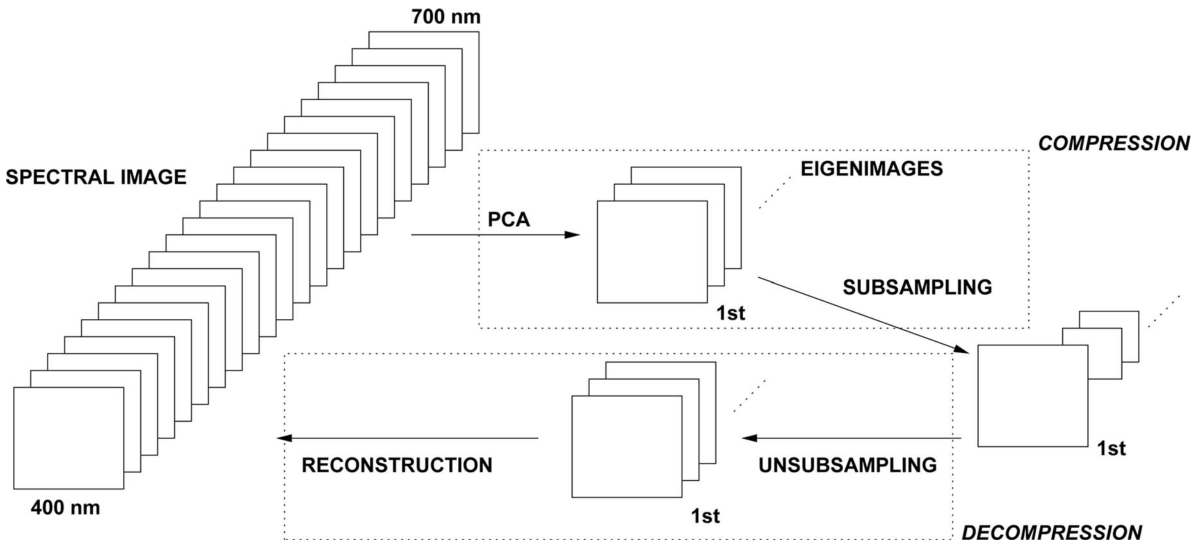

Figure 5. Schematic presentation of subsampled image formation.

Fig. 4, the original image and the inner products between the original spectral image and these eigenvectors, i.e., the eigenimages, are shown.

In this study, we apply the subsampling methodology into all the other eigenimages except the first one. Due to the accuracy requirements mentioned above, one may need more than three eigenimages for spectral image reconstruction. Therefore, we expand the subsampling into more than two eigenimages.

In the spectral image archive, the images are stored either in raw spectral image format or directly as a set of eigenimages. In browsing, the image is sent from the server to the client using a subsampling filter. In the case of the raw spectral image, the filter first computes the eigenimages. In the case of the eigenimage format these images are read directly from the image archive. Then the first eigenimage is transferred as such, and the other eigenimages are subsampled using a subsampling scheme.

At the client end, the image is reconstructed by expanding the subsampled eigenimages into the original size and combining the reconstructed spectral image from the eigenimages. The number of eigenimages and the subsampling scheme depend on the spectral accuracy requirements and the data communication bandwidth. From this reconstructed spectral image, the final displayed multiprimary, RGB, or printed image is formed by a display filter. The process of subsampled image formation is shown schematically in Fig. 5.

In this scheme, we first compute the eigenvectors from the whole image, form the full size eigenimages, and do subsampling for those eigenimages. It is worth it to consider if it would be computationally more effective to do subsampling already for the raw image components. All symbols of this computation are listed in Table III.

Table III. Symbols.

Symbols	
C_1, C_2	Compressed multispectral image
I	Original multispectral image; pixels are ordered to a vector
I_s	Subsampled multispectral image
P_1, P_2	Vector of m eigenvectors produced by PCA
P_1^*, P_2^*	Vector of m-1 eigenvectors, without τ_1
S_1, S_2	Set of subsampled eigenimages
k	Number of pixels in the image
k'	Number of pixels in the subsampled image
m	Number of eigenimages
n	Dimension of spectrum
δ	Delta-function, which chooses the pixels for subsampling
τ_i	ith eigenvector
$X \rightarrow Y$	X approaches to Y

Let $I(x)$ be the spectral image with k pixels, where the pixels are ordered to a vector, and each pixel value $I(x_i)$ is a n-dimensional color spectrum. The PCA eigenimages can be presented as projections $PI(x)$, where P is a vector of eigenvectors $\tau_1, \ldots, \tau_n$ produced by the PCA method from the pixels spectra. Let S be the set of all pixels in the image and S_i a subset of pixels. The subsampling of a spectral image can now be represented as

Table IV. The spectral reconstruction errors for the CORAL database containing ten spectral images. In the first column, m denotes the number of component images used.

m	MSD	PSNR	ΔE_{avg}	$\Delta E_{S\text{-}CIELAB}$	Fidelity
1	46.53	29.50	8.24	7.43	97.17
2	27.06	34.60	4.60	3.73	99.12
3	18.81	37.72	3.00	2.15	99.59
4	14.86	39.98	2.02	1.29	99.75
5	12.09	41.90	1.51	0.89	99.84
6	10.21	43.45	1.15	0.59	99.91
7	8.89	44.68	0.96	0.45	99.93
8	7.76	45.89	0.65	0.30	99.95
9	6.82	47.02	0.48	0.23	99.96
10	5.93	48.28	0.36	0.16	99.97

Table V. The spectral reconstruction errors for the FOREST database containing 12 spectral images. In the first column, m denotes the number of component images used.

m	MSD	PSNR	ΔE_{avg}	$\Delta E_{S\text{-}CIELAB}$	Fidelity
1	33.50	32.40	7.30	5.57	98.14
2	19.83	36.88	3.36	2.44	99.34
3	12.44	41.39	1.53	1.01	99.76
4	8.75	44.57	1.03	0.58	99.89
5	6.75	46.93	0.70	0.34	99.94
6	5.65	48.62	0.50	0.24	99.97
7	4.87	49.94	0.31	0.12	99.98
8	4.30	51.10	0.24	0.08	99.98
9	3.85	52.11	0.21	0.06	99.98
10	3.45	53.09	0.19	0.06	99.99

$$S_i = \delta(x_i - x_0)PI(x), \tag{1}$$

where $\delta(x)$ is the delta function and (x_i) goes over of a subset of pixels. Let us also define that this subset contains k' pixels.

Let us define that P_1 is a vector of eigenvectors $\tau_1, \dots, \tau_m$, where m is the number of eigenimages used in the image representation. Let also P_1^* be the vector of eigenvectors, where the first eigenvector τ_1 has been removed from the P_1. Now we have eigenvectors $\tau_2, \dots, \tau_m$ in P_1^*. The subsampled set of eigenimages is

$$S_1 = \delta(x_i - x_0)P_1^* I(x), \tag{2}$$

where (x_i) goes over of a subset of pixels. When these subsets are chosen as shown in Fig. 2, we get different subsampling schemes. Now

$$C_1 = (\tau_1^T I) \cup S_1 \tag{3}$$

form the set of eigenimages sent to the client, where C_1 is the compressed multispectral image.

There are three questions to consider: can we change the order of subsampling and projection operation, how to estimate P, and what are the most efficient subsampling schemes.

For increasing the computational efficiency, we consider the change of order of subsampling and projection operation. This means that we compute the eigenvectors from the subsampled raw images. Now the set S_1 in Eq. (2) is replaced by the set

$$S_2 = P_2^*(\delta(x_i - x_0)I_s(x)), \tag{4}$$

where P_2^* is vector of eigenvectors estimated from the subsampled image I_s.

Table VI. The average $\Delta E_{S\text{-CIELAB}}$ errors and PSNR in reconstruction for the CORAL database (ten spectral images).

CORAL	MSD	PSNR	$\Delta E_{S\text{-CIELAB}}$
PCA 4:4:4	18.81	37.72	2.15
PCA 4:2:2	22.49	35.58	2.29
PCA 4:2:0	25.59	34.18	2.50
PCA 4:1:1	27.16	33.44	2.69

Table VII. The average $\Delta E_{S\text{-CIELAB}}$ errors and PSNR in reconstruction for the FOREST database (12 spectral images).

FOREST	MSD	PSNR	$\Delta E_{S\text{-CIELAB}}$
PCA 4:4:4	12.44	41.39	1.01
PCA 4:2:2	17.28	37.94	1.31
PCA 4:2:0	21.76	35.87	1.71
PCA 4:1:1	23.57	34.97	2.15

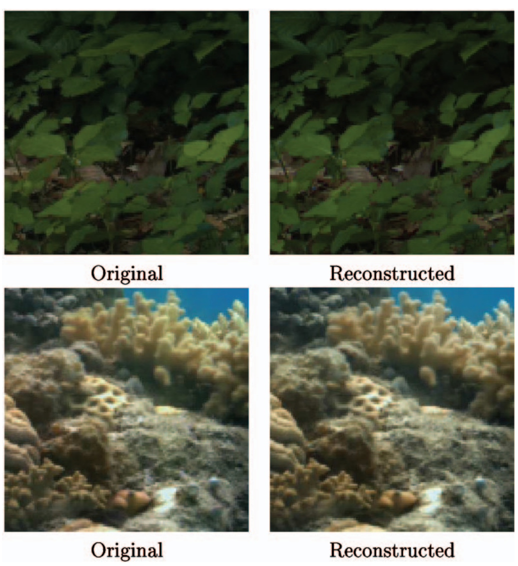

Figure 6. Two examples of original and reconstructed browser image.

The set of image components to be sent to the client is now

$$C_2 = (\tau_1^T I) \cup S_2, \tag{5}$$

where τ_1^T is the first PCA eigenvector of subsampled images.

It is obvious that

$$C_2 \rightarrow C_1 \tag{6}$$

when

$$P_2 \rightarrow P_1 \tag{7}$$

and the sets C_1 and C_2 are equal if P_1 and P_2 are estimated from the same set of pixels.

Algorithms for the two procedures above, Eqs. (2) and (4), are as follows:

ALGORITHM 1

1. Form correlation matrix
$n \times n$ matrix using k pixels $O(kn^2)$

2. Compute eigenvectors
m eigenvectors $O(n^3 + (n \log^2 n)\log b)$ within relative error bound 2^{-b}, see Ref. 33

3. Compute inner product images
k pixels, m component images $O(knm)$

4. Subsample image
$m-1$ component images $O(k'(m-1))$ or $O(k(m-1))$ depending on the method

ALGORITHM 2

1. Subsample image
n component images $O(k'n)$ or $O(kn)$ depending on the method

2. Form correlation matrix
$n \times n$ matrix using subset of pixels $O(k'n^2)$

3. Compute eigenvectors
m eigenvectors $O(n^3 + (n \log^2 n)\log b)$ within relative error bound 2^{-b}, see Ref. 33

4. Compute inner product images
k pixels for first eigenimage, for sub sampled pixel set $m-1$ component images $O(kn + k'n(m-1))$

Algorithm 2 is computationally more efficient. The efficiency is based on the following steps:

1. The correlation matrix is formed from a smaller set of pixels (step 2). When comparing to this, the increment of component images for subsampling (step 1) is not relevant.
2. A smaller number of inner products computed for eigenimages (step 4). The benefit is dependent on the subsampling scheme.

The vector of projections P for each image can be computed from all pixels in the image or estimated from a subset of pixels. In Algorithm 2 (step 2), this subset is chosen by subsampling scheme. It is also possible to use random subset in both algorithms.

Figure 2 shows the common subsampling schemes. Since we are considering spectral images, we may use more than three eigenimages. Therefore, we have studied new schemes for subsampling including mean of subsampling window. This would give us the possibility to use more eigenimages for more accurate color with the same data transmission bandwidth. The mean or median of pixel vectors are motivated estimates if we consider that the pixel distribution function is with normal density or Laplace distribution, respectively.[34]

In the previous treatment of images, the PCA eigenvectors can be replaced by ICA basis vectors.[28]

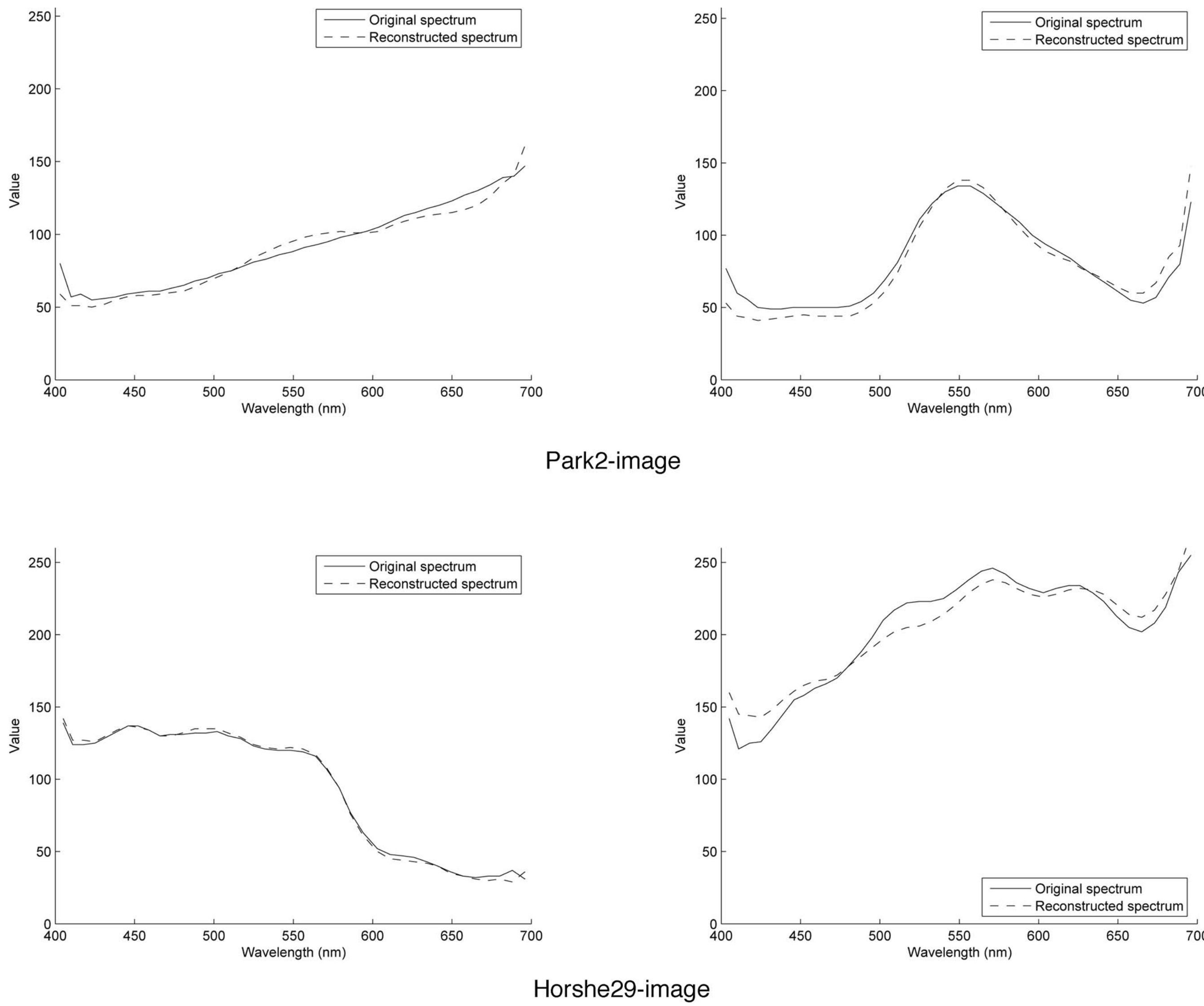

Figure 7. Examples of spectra in original (solid) and reconstructed (dashed) browser image.

Table VIII. The average $\Delta E_{S\text{-}CIELAB}$ errors in reconstruction for the FOREST database containing 12 spectral images. The block size 3×3 pixels were used in subsampling and the block was represented by the center vector or the average vector. The results are reported for 3, 4, and 5 eigenimages.

FOREST		3×3 center			3×3 average	
Number of eigenimages	3	4	5	3	4	5
$\Delta E_{S\text{-}CIELAB}$	2.02	1.81	1.73	1.47	1.16	1.04

EXPERIMENTAL RESULTS

To test the proposed method, we used FOREST and CORAL spectral image databases acquired by Chiao et al.[32] FOREST and CORAL databases contain 12 and 10 spectral images, respectively. The images were acquired in the range of 403–696 nm using an interference filter based spectral camera system. The spectral images contain 40 channels.

First, the PCA was applied for each spectral image individually in both databases. The same 128×128 central part of the image was used as in the study of Chiao et al.[32] The image quality at the browser was measured as spectral error between original and reconstructed spectral image. The following error measures were used:

Fidelity: measures the amount of information in m eigenvectors.

Table IX. The CR for the CORAL and FOREST databases used in our experiments.

Number of eigenimages	Method (block size)	CR
3	4:4:4 (2×2)	13.3
3	4:2:2 (2×2)	19.9
3	4:2:0 (2×2)	26.5
3	4:1:1 (1×4)	26.5
3	(3×3)	32.4
4	(3×3)	29.7
5	(3×3)	27.3

Mean Spectral Distance (MSD): mathematical error of values. This is the average euclidean distance between original and reconstructed image.

Peak Signal-to-Noise Ratio (PSNR): measures the noise in the image.

$\boldsymbol{\Delta E}$ and $\boldsymbol{\Delta E}_{S\text{-CIELAB}}$: is used as a human visuality measure. This measures the color difference between the images. S-CIELAB is a spatial extension of CIELAB proposed by Zhang and Wandell.[35] Here, standard D65 was used as a light source.

We computed the results using up to ten eigenimages. These results are collected in Tables IV and V. It can be seen that 3–5 eigenimages are needed for the series to achieve adequate results. There is no subsampling used in this compression.

The Fidelity, MSD, and PSNR error measures are calculated as follows:

$$\text{Fidelity} = 100\frac{\sum_{i=1}^{m} \tau_i}{\sum_{j=1}^{n} \tau_j}, \tag{8}$$

$$\text{MSD} = \frac{1}{k}\sum_{i=1}^{k} \sqrt{\sum_{j=1}^{n} (o_j - r_j)^2}, \tag{9}$$

$$\text{PSNR} = 10 \log_{10} \frac{255^2}{\text{MSE}}, \tag{10}$$

where o_i is the original channel value, r_i is the reconstructed channel value, and MSE is the mean squared error.

Algorithms 1 and 2 were programmed in MATLAB on UNIX platform for all subsampling schemes shown in Fig. 2. The spectral image reconstruction results are shown in Tables VI and VII. In the 4:4:4 subsampling scheme, there is no spatial compression done, i.e., the reconstruction corresponds to PCA spectral reconstruction.[24] Here, three eigenimages were used in the compression. There is greater variety in hue in CORAL-database images than in FOREST-database images, which makes the average errors higher in the CORAL database. The original and reconstructed browser images were also compared visually on the computer display. Two examples of these image pairs are shown in Fig. 6 with the 4:2:0 subsampling scheme. A couple of examples of the original (solid) and reconstructed (dashed) spectra from these images are shown in Fig. 7, where the calculated ΔE is near the average.

In the following experiments, we used more eigenimages to represent the spectral domain and to keep the compression ratio (CR) in a reasonable level, the block size in subsampling was enlarged to 3×3 pixels. The vector, which represents the 3×3 pixels block, was first selected from the center pixel of the block. Also the mean vector of the 3×3 pixels block was tested. The results for the FOREST database are collected in Table VIII. Using the average vector, the reconstruction accuracy was improved. The compression ratios for all the compressions performed are shown in Table IX. The compression ratio is calculated as follows:

$$\text{CR} = \frac{\text{size of original image (bytes)}}{\text{size of compressed image (bytes)}}. \tag{11}$$

The size of the compressed image in Eq. (11) contains the size of subsampled eigenimages and also the size of eigenvectors, which are needed for image reconstruction. The examples of the theoretical time required for transferring the original and compressed images via network are collected in Table X.

DISCUSSION

In the present study, we addressed the problem of browsing spectral image archives. A browsing architecture is proposed and considered the problem of fast image transmission from the server to the client computer. It is assumed that in browsing, the accurate spectral information is not needed, but the images should have acceptable visual quality. By reconstructing the spectral image in the client side, it can be tuned for the wanted display by the display filter.

In the server, the images may be stored in raw spectral image format or in PCA spectral image format. Also the ICA format can be used. PCA and ICA formats are device independent data formats. We experimented also with ICA based spectral compression and concluded that the performance of PCA and ICA in compression were almost similar.

We first used PCA to reduce the number of component images and then the subsampling schemes used in JPEG and MPEG type color image compression were applied for PCA based component images. Also another approach, which first subsamples the spectral image and then calculates PCA for the subsampled image was discussed and tested. The reconstruction errors were similar in both algorithms. This is because the difference between the algorithms is that, statistically, in algorithm 2 there are fewer spectra used for calculating the correlation matrix in PCA. Therefore, there may be small differences between the eigenvectors of the

Table X. Examples of theoretical time required for transferring images via network.

Format	Image size	28800 bps	56000 bps	128000 bps	512000 bps
Original image[a]	655360 B	3 min	1.5 min	41.0 s	10.2 s
4:4:4	49272 B	13.7 s	7 s	3.1 s	0.8 s
4:2:0	24696 B	6.9 s	3.5 s	1.5 s	0.4 s
Original image[b]	63963136 B	4.9 h	2.5 h	1.1 h	16.7 min
4:4:4	3145911 B	14.6 min	7.5 min	3.3 min	49 s
4:2:0	1573047 B	7.3 min	3.7 min	1.6 min	25 s

[a] 128×128 pixels, 40 channels.
[b] 1024×1024 pixels, 61 channels.

algorithms and this can lead to small differences in spectral image reconstruction. Algorithm 2 was computationally about 10% faster than algorithm 1. The CPU times needed for compressing and decompressing the FOREST database containing 12 spectral images were 178 s for algorithm 1 and 159 s for algorithm 2. When the block size is constant for each channel, then algorithm 2 can be applied. However, for example, if the block size for the second eigenimage is 2×2 and 3×3 for the third eigenimage, then algorithm 2 cannot be applied.

The searching of images from the archive was not included in this study. However, if the client user has a spectral image and wants to search for a similar image from the spectral image database, one possibility is that the client calculates the eigenvectors for a spectral image and then the search is done by comparing the eigenvectors for images in the database. This-way the images with similar spectral characteristics can be searched. When the desired image is found by browsing, then the raw spectral image can be downloaded, for example, for computational purposes where the accurate spectral and spatial resolution are needed.

Our experiments show that the proposed compression method is suitable for browsing, i.e., for visual purposes. The browsed image can be tuned to a desired display device, including also a multiprimary display. The error calculations ($\Delta E_{S\text{-CIELAB}}$ values) are in a reasonable level. If more eigenimages are employed in spectral representation then the spectra are more accurate, but in order to keep the compression ratio at a suitable level, the block size could be then made larger. For example, in Table IX the CR for 5 eigenimages (3×3 block) is 27.3 and for three eigenimages (method 4:2:0) the CR is 26.5, i.e., they are compressed images with the same size. However, the $\Delta E_{S\text{-CIELAB}}$ value for five eigenimages (1.04) is lower than for three eigenimages (1.71). The analysis of the optimal number of eigenimages versus the optimal block size needs to be further investigated. In Table X, the advantage of the proposed compression in network transfer can be clearly seen.

ACKNOWLEDGMENTS

The authors thank Chuan-Chin Chiao for the spectral image databases, Brian Wandell and Xuemei Zhang for S-CIELAB programs and discussions, and Lindsay MacDonald for discussions.

REFERENCES

1 T. Ajito, T. Obi, M. Yamaguchi, and N. Ohyama, "Six-primary color projection display for expanded color gamut reproduction", in *Proceedings, International Symposium on Multispectral Imaging and Color Reproduction* (Chiba University, Chiba, Japan, 1999), pp. 135–138.

2 L. W. MacDonald and M. R. Luo, *Colour Image Science* (Wiley, London, 2002).

3 G. Wyszecki and W. S. Stiles, *Color Science: Concepts and Methods, Quantitative Data and Formulae*, 2nd ed. (Wiley, New York, 1982).

4 M. Hauta-Kasari, J. Parkkinen, T. Jaaskelainen, and R. Lenz, "Spectral based analysis of color images", in *Proceedings, 8th Congress of the International Colour Association, AIC Color 97, Vol. II* (AIC, Kyoto, Japan, 1997)), pp. 548–551.

5 S. Kawata, K. Sasaki, and S. Minami, "Component analysis of spatial and spectral patterns in multispectral images. I. Basis", J. Opt. Soc. Am. A **4**, 2101–2106 (1987).

6 S. Tominaga, "Spectral imaging by a multispectral camera", J. Electron. Imaging **8**, 332–341 (1999).

7 C. C. Hoyt, "Toward higher res, lower cost quality color and multispectral imaging", Adv. Imaging Electron Phys. 53–55 (1995).

8 T. Hyvärinen, E. Herrala, and A. Dall'Ava, "Direct sight imaging spectrograph: A unique add-on component brings spectral imaging to industrial applications", Proc. SPIE **3302**, 21 (1998).

9 M. Hauta-Kasari, K. Miyazawa, S. Toyooka, and J. Parkkinen, "Spectral vision system for measuring color images", J. Opt. Soc. Am. A **16**, 2352–2362 (1999).

10 K. Miyazawa, M. Hauta-Kasari, and S. Toyooka, "Rewritable broad-band filters for color image analysis", Proc. SPIE **3740**, 468–471 (1999).

11 J. Hallikainen, J. P. S. Parkkinen, and T. Jaaskelainen, "Color Image Processing with AOTF", *Proceedings, 6th Scandinavian Conference on Image Analysis* (Pattern Recognition Society of Finland, Oulu, Finland, 1989), pp. 294–300.

12 K. Itoh, "Interferometric multispectral imaging", in *Progress in Optics XXXV*, edited by E. Wolf (Elsevier Science, Amsterdam, 1996), pp. 145–196.

13 H. Motomura, N. Ohyama, M. Yamaguchi, H. Haneishi, K. Kanamori, and S. Sannohe, "Development of six-primary HDTV-display system", *Proceedings, 22nd International Display Research Conference, Eurodisplay 2002* (Publisher, Place, 2002), pp. 563–566.

14 F. H. Imai, M. R. Rosen, D. Wyble, R. Berns, and D. Tzeng, "Spectral reproduction from scene to hardcopy I: Input and output", Proc. SPIE **4306B**, 346–357 (2001).

15 P. Koponen, H. Kälviäinen, and J. Parkkinen, "Multispectral video", *Proceedings, 15th International Conference on Pattern Recognition, ICPR-2000*, Vol. 3 (IEEE Press, Barcelona, Spain, 2000), pp. 190–193.

16 K. Ohsawa, T. Ajito, Y. Komiya, H. Haneishi, M. Yamaguchi, and N. Ohyama, "Six band HDTV camera system for spectrum-based color reproduction", J. Imaging Sci. Technol. **48**, 85–92 (2004).

17 Softcolor, "Softcolor Oy Ltd. awarded in 2005 INNOFINLAND competition", http://www.softcolor.fi/index.php?page=news&id=3011 (accessed Feb. 25, 2006).

[18] K. Martinez, J. Cupitt, D. Saunders, and R. Pillay, "Ten years of art imaging research", Proc. IEEE **90**, 28–41 (2002).

[19] M. Nishibori, "Problems and solutions in medical color imaging", *Proceedings, Second International Symposium on Multispectral Imaging and High Accurate Color Reproduction* (Chiba University, Chiba, Japan, 2000), pp. 9–17.

[20] L. W. MacDonald, S. Westland, and J. Shaw, "Colour image reproduction: Spectral vs spatial", *Proceedings, International Symposium on Multispectral Imaging and Color Reproduction* (Chiba University, Chiba, Japan, 1999), pp. 81–91.

[21] M. Hauta-Kasari, J. Lehtonen, J. Parkkinen, and T. Jaaskelainen, "Representation of spectral images in data communications", Proc. SPIE **4421**, 500–503 (2002).

[22] F. König and W. Praefcke, "Multispectral image encoding", *Proceedings, IEEE International Conference on Image Processing* Vol. 3 (IEEE, Piscataway, NJ, 1999), pp. 123–126.

[23] W. Kondou, K. Miyata, H. Haneishi, and Y. Miyake, "An evaluation of image quality for compressed multi-spectral image", *Proceedings, International Symposium on Multispectral Imaging and Color Reproduction* (Chiba University, Chiba, Japan, 1999), pp. 143–146.

[24] J. P. S. Parkkinen, J. Hallikainen, and T. Jaaskelainen, "Characteristic spectra of Munsell colors", J. Opt. Soc. Am. A **6**, 318–322 (1989).

[25] L. T. Maloney, "Evaluation of linear models of surface spectral reflectance with small numbers of parameters", J. Opt. Soc. Am. A **3**, 1673–1683 (1986).

[26] J. A. Saghri, A. G. Tescher, and J. T. Reagan, "Practical transform coding of multispectral imager", IEEE Signal Process. Mag. **12**, 32–43 (2005).

[27] A. Hyvärinen, J. Karhunen, and E. Oja, *Independent Component Analysis* (Wiley, New York, 2001).

[28] T. Wachtler, T.-W. Lee, and T. J. Sejnowski, "Chromatic structure of natural scenes", J. Opt. Soc. Am. A **18**, 65–77 (2001).

[29] T. Keusen and W. Praefcke, "Multispectral color system with an encoding format compatible to the conventional tristimulus model", *Proc., IS & T/SID 3rd Color Imaging Conference* (IS&T, Springfield, VA, 1995).

[30] P. K. Kaiser and R. M. Boynton, *Human Color Vision*, 2nd ed. (Optical Society of America, Washington, DC, 1996).

[31] C.-H. Wu and J. D. Irwin, *Emerging Multimedia Computer Communication Technologies* (Prentice-Hall, Englewood Cliffs, NJ, 1998).

[32] C.-C. Chiao, T. W. Cronin, and D. Osorio, "Color signals in natural scenes: Characteristics of reflectance spectra and effects of natural illuminants", J. Opt. Soc. Am. A **17**, 218–224 (2000).

[33] V. Y. Pan and Z. Q. Chen, "The complexity of the matrix eigenproblem", *Proceedings, 31st Annual ACM Symposium on Theory of Computing* (ACM, Atlanta, Georgia, 1999), pp. 507–516.

[34] J. Astola and P. Kuosmanen, *Fundamentals of Nonlinear Digital Filtering* (CRC Press, Boca Raton, FL, 1997).

[35] X. Zhang and B. A. Wandell, "A spatial extension of CIELAB for digital color image reproduction", Proc. SID **5**, 61–63 (1997).